NAVAL SHIP RESEARCH AND DEVELOPMENT CENTER
Bethesda, Maryland 20034

LAMINAR FLOW PAST BODIES UNDER PERFECT SLIP

Hans J. Lugt

Approved for public release; distribution unlimited.

COMPUTATION AND MATHEMATICS DEPARTMENT

July 1973 Report 4227

LAMINAR FLOW PAST BODIES UNDER PERFECT SLIP

The Naval Ship Research and Development Center is a U. S. Navy center for laboratory effort directed at achieving improved sea and air vehicles. It was formed in March 1967 by merging the David Taylor Model Basin at Carderock, Maryland with the Marine Engineering Laboratory at Annapolis, Maryland.

Naval Ship Research and Development Center
Bethesda, Md. 20034

MAJOR NSRDC ORGANIZATIONAL COMPONENTS

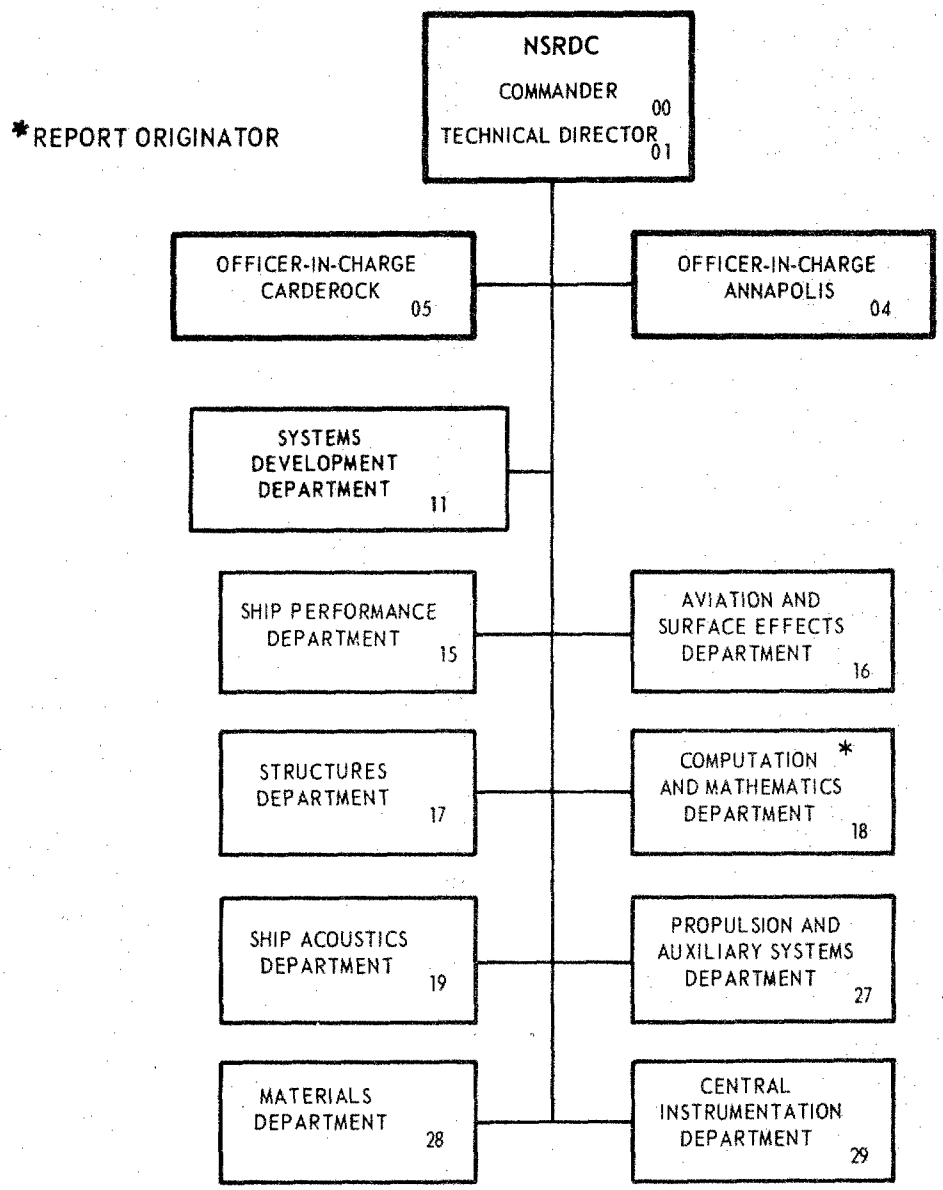

NDW-NSRDC 3960/44 (REV. 8/71)
GPO 917-872

DEPARTMENT OF THE NAVY
NAVAL SHIP RESEARCH AND DEVELOPMENT CENTER
Bethesda, Maryland 20034

LAMINAR FLOW PAST BODIES UNDER PERFECT SLIP

by

Hans J. Lugt

July 1973

Report 4227

TABLE OF CONTENTS

LIST OF FIGURES

NOTATION

a	Focal distance of the elliptic body contour
A, B	Integration constants defined in Equation (4)
C_D	Drag coefficient
C_{DF}, C_{DP}	Drag coefficient due to friction, pressure
d	Width of the ellipse = a cosh η_1
K	Constant defined in Equation (5)
n, s	Intrinsic coordinates
p	Pressure
r, ϕ	Spherical polar coordinates in the meridional plane
Re	Reynolds number = $dU\rho/\mu$
s'	Wake length
t'	Time
t	Dimensionless time = $t'U/a$
v_θ	Surface velocity made dimensionless by U
x, y	Cartesian coordinates
u	Velocity component along streamline
U	Constant velocity far away from the body
α	Angle of attack
η, θ	Elliptic coordinates, $x + iy = a \cosh(\eta + i\theta)$
$\bar{\eta}, \bar{\theta}$	Oblate spheroidal coordinates, $x + iy = a \sinh(\bar{\eta} + i\bar{\theta})$
κ	Curvature of streamlines
μ	Dynamic viscosity
ρ	Density
τ	Shear stress along streamline
ψ	Stream function
ω	Vorticity
Subscript	
1	Body surface

ABSTRACT

Current experiments conducted at Dornier System on special solid-surface treatment have prompted a study on the fluid dynamic implications of perfect-slip flow. Numerical results on incompressible fluid flows past thin elliptic cylinders at various angles of attack and at moderate Reynolds numbers show that flow separation, instability, and vortex shedding occur also under the perfect-slip condition. Of particular interest is the generation and spreading of an initial vortex after the abrupt start of an airfoil. The circulation theory of lift for potential flows is also applicable to perfect slip. Thus, lift exists so that flying under perfect slip is possible.

ADMINISTRATIVE INFORMATION

This study was funded by the Naval Ship Systems Command under the Mathematical Sciences Program, Subproject SR 014 03 01, Work Unit 1-1843-347.

This report is a reprint of the paper "Laminar Flow Past Bodies Under Perfect Slip," published in the proceedings of the "Symposium über Gas-Oberflächen-Wechselwirkung," May 3-5, 1972, Meersburg, Lake Constance, Germany, sponsored by the German Ministry of Defense and organized by Dornier System, Friedrichshafen.

INTRODUCTION

A few years ago Sydney Goldstein remarked that, if a fluid could slip freely over the surface of a solid body, the world would be very different.[1] Would it really be? To give a partial answer to this question some computer experiments have been made which simulate a viscous fluid flowing past a cylindrical body under the perfect-slip condition. Perfect slip is the limiting case of slippage when the shear stress at the solid surface vanishes. This is a hypothetical situation since slip flow of a Newtonian fluid still awaits verification in reality. Only the availability of electronic computers enables us to simulate such an imaginary flow. It is not the purpose of this paper to argue about whether and how slip flow can be obtained within the realm of continuum physics where the mean free path is very small with respect to the body length. Apart from problems in the rarefied-gas regime or from certain cases of non-Newtonian liquids (for instance, Bingham bodies) where slippage is known to exist, a renewed interest has arisen in how to obtain slip flow for a Newtonian continuum. An outgrowth of this effort is the present Symposium. Interest in such a slip flow was also the incentive for this study. Some numerical results on vorticity production and propagation under perfect slip have been published already.[2]

---

[1] References are listed on page 17.

VORTICITY PRODUCTION ON THE BODY

In a homogeneous incompressible fluid without nonconservative forces acting, vorticity can be produced only at the body surface. By using intrinsic coordinates s, n for plane or axisymmetric motions, where s coincides with the streamlines, and n is orthogonal to s, the vorticity ω and the shear stress τ on a streamline are functions of the velocity u along n = const:

$$\omega = -\frac{\partial u}{\partial n} + \kappa u \ , \tag{1}$$

$$\tau/\mu = -\frac{\partial u}{\partial n} - \kappa u \ , \tag{2}$$

where μ is the dynamic viscosity and κ the curvature of the streamline. Under the nonslip condition, $u \equiv 0$ at the body surface $n = n_1$, Equations (1) and (2) reduce to $\omega = \tau/\mu = -\partial u/\partial n$. Under the perfect-slip condition, $\tau \equiv 0$ on $n = n_1$, the vorticity is $\omega = 2\kappa u$. Hence, vorticity occurs at the surface under perfect slip only for $\kappa \neq 0$. Since every cylindrical body with a closed line contour of its cross-section, and every axisymmetric body with a closed surface contour, must have areas (or points) with nonvanishing curvature, vorticity will always be generated under perfect slip at those bodies.

The rate of transport of vorticity from the surface $n = n_1$ into the fluid is proportional to $(\partial\omega/\partial n)_1$. This term, and not the vorticity ω_1 itself, enters the equation for the surface pressure p_1 and, hence, participates in determining drag, lift, and torque. The relation between p_1 and $(\partial\omega/\partial n)_1$ follows from the s-component of the Navier-Stokes

equation:

$$p_1 = p_{const} - \int_{surface} \left[\rho\left(\frac{\partial u}{\partial t'} + u\,\frac{\partial u}{\partial s}\right) + \mu\,\frac{\partial \omega}{\partial n}\right] ds\ , \qquad (3)$$

where ρ is the density of the fluid and t' the time. Under perfect slip the term $(\partial\omega/\partial n)_1$ can differ from zero on a flat part of the surface, where $\kappa = 0$ and therefore $\omega_1 = 0$. In this case vorticity inside the fluid is provided from other areas of the surface where $\kappa \neq 0$. The only case for which $\omega_1 \neq 0$ but $(\partial\omega/\partial n)_1 \equiv 0$ is the solid-body rotation. No exchange of vorticity takes place. The vorticity is "frozen" inside the fluid. There is no dissipation.

Two well-known analytic solutions may illustrate the role of vorticity production in determining drag. For the steady flow past a sphere of unit radius at vanishing Reynolds number $Re = 2U\rho/\mu$, the stream function ψ and the azimuthal vorticity ω are

$$\psi = -\frac{U}{2}\sin^2\phi\,\left(Ar + \frac{B}{r} + r^2\right), \qquad \omega = \frac{AU}{r^2}\sin\phi\ , \qquad (4)$$

where r, ϕ are the spherical polar coordinates in the meridional plane. U is the velocity at infinity. The integration constants A and B are $A = -3/2$, $B = 1/2$ for nonslip and $A = -1$, $B = 0$ for perfect slip.[3] The drag coefficient C_D (the sum of C_{DF} and C_{DP}, where C_{DF} and C_{DP} are the portions due to friction and pressure, respectively) is defined by $C_D = \text{Drag}/(\rho/2)\pi U^2$. Then, for

Nonslip: $\quad C_D Re = 24,\ C_{DF} Re = 16,\ C_{DP} Re = 8\ ,$

Perfect slip: $\quad C_D Re = 16,\ C_{DF} Re = 0,\ C_{DP} Re = 16.$

Hence, the total drag coefficient for perfect slip is tremendous, 2/3 that for nonslip. C_{DP} itself is even twice as large for perfect slip

although $(\partial\omega/\partial r)_1$ is smaller. The larger C_{DP}-value is due to the contribution of the surface velocity in Equation (3).

If the sphere is flattened to an oblate spheroid, an analytic solution for vanishing Reynolds number exists (Oberbeck solution[3]). In oblate spheroidal coordinates $\bar{\eta}$, $\bar{\theta}$ for the meridional plane with $x + iy = a \sinh(\bar{\eta} + i\bar{\theta})$, ψ and ω are, for nonslip,

$$\psi = \frac{U \cosh^2 \bar{\eta}}{2 \cosh^2 \bar{\eta}_1} \sin^2 \bar{\theta} \left[1 - \frac{1}{K} \left(\frac{\sinh \bar{\eta}}{\cosh^2 \bar{\eta}} - \frac{\sinh^2 \bar{\eta}_1 - 1}{\cosh^2 \bar{\eta}_1} \cot^{-1} \sinh \bar{\eta}\right)\right], \tag{5}$$

$$\omega = \frac{2U \sin \bar{\theta}}{K \cosh \bar{\eta}_1} \quad \frac{\tanh \bar{\eta}}{\cosh^2 \bar{\eta} - \sin^2 \bar{\theta}},$$

where the focal distance a is chosen in such a way that the oblate spheroid has unit radius, that is, $a = 1/\cosh \bar{\eta}_1$. The surface of the body is $\bar{\eta} = \bar{\eta}_1$. The constant K is

$$K = \frac{1}{\cosh^2 \bar{\eta}_1} \left[\sinh \bar{\eta}_1 - (\sinh^2 \bar{\eta}_1 - 1) \cot^{-1} \sinh \bar{\eta}_1\right].$$

For the flat disk $\bar{\eta}_1 = 0$ we observe the following curious situation: Except at the edge the surface vorticity is zero and, therefore, the shear stress is zero, whereas $(\partial\omega/\partial\bar{\eta})_1 \neq 0$ in general. The total vorticity field is generated at the focal point which for $\bar{\eta}_1 = 0$ coincides with the edge. The situation is illustrated in Figure 1 for the fat oblate spheroid $\bar{\eta}_1 = 0.5$ to show the lines of constant vorticity inside the body. Notice that $(\partial\omega/\partial\bar{\eta})_1$ changes its sign along the surface. Near the centerline vorticity is transported from the fluid to the body. Around the edge vorticity emanates from the surface. For $\bar{\eta}_1 = 0$ this region is confined to the edge.

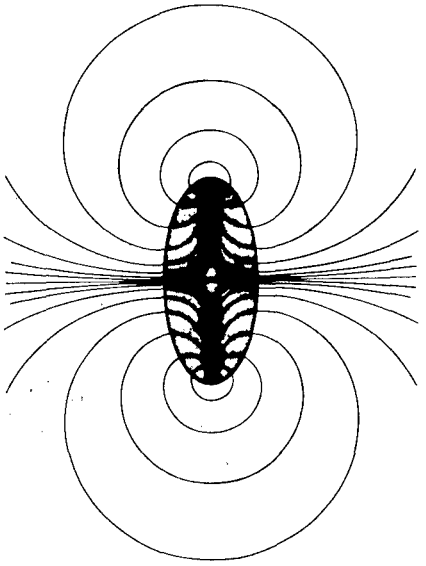

Figure 1. Lines of Constant Vorticity for an Oblate Spheroid $\bar{\eta}_1 = 0.5$ at Re = 0 Under Nonslip

Under the perfect-slip condition the solution is not separable, and an analytic integral could not be obtained. A numerical solution was therefore constructed for $\bar{\eta}_1 = 0.05$. (The numerical procedure breaks down for $\bar{\eta}_1 = 0$.) The drag coefficients are:

Nonslip, $\bar{\eta}_1 = 0$: $C_D Re = 20.372$, $C_{DF} = 0$,

Nonslip, $\bar{\eta}_1 = 0.05$: $C_D Re = 20.395$, $C_{DF} = 1.504$,

Perfect slip, $\bar{\eta}_1 = 0.05$: $C_D Re \approx 28$, $C_{DF} = 0$.

Although the numerical value for perfect slip is very crude, the result shows that, as in the case of the sphere flow, C_{DP} is greater for perfect slip than for nonslip.

FLOW BEHAVIOR UNDER PERFECT SLIP

The study of flows past bodies for nonvanishing Reynolds numbers requires the use both of numerical methods and of electronic computers. An existing computer code[4] for moderate Reynolds numbers has been employed to calculate two-dimensional laminar flows of an incompressible fluid past elliptic cylinders under perfect slip. Some data have been published already[2] so that the results reported here may be considered as complements.

In this computer code the elliptic cylinder is imbedded in a network of points which are the intersections of constant elliptic coordinate lines. The elliptic coordinates η, θ are related to the Cartesian coordinates x, y by

$$x + iy = a \cosh(\eta + i\theta), \quad a > 0, \tag{6}$$

where a is the focal distance. The body contour is given by $\eta = \eta_1$ (Figure 2).

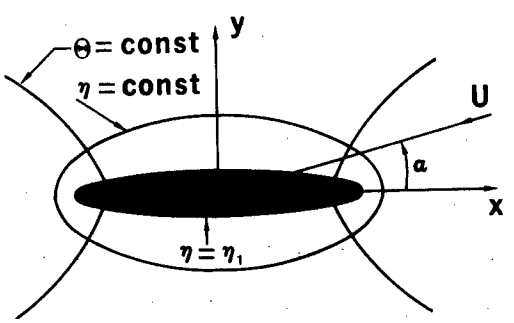

Figure 2. Elliptic Coordinate System and Definition of Angle of Attack α.

The Reynolds number is defined by $Re = dU\rho/\mu$ with $d = a \cosh \eta_1$. The calculation starts with a potential flow as initial condition at $t = t'U/a = 0$.

The following examples have been selected:

$\alpha = 0^{\circ}$, $Re = 200$, $\eta_1 = 0.1$, symmetric, almost steady flow

$\alpha = 90^{\circ}$, $Re = 10$, $\eta_1 = 0.1$, symmetric, almost steady flow

$\alpha = 45^{\circ}$, $Re = 200$, $\eta_1 = 0.05$, asymmetric, transient flow

Flows past thin elliptic cylinders under perfect slip show the largest divergence from those under nonslip when $\alpha = 0^{\circ}$. The reason is that, under nonslip, friction drag predominates over pressure drag. Under perfect slip, however, friction drag is zero by definition. For $\alpha = 0^{\circ}$, $Re = 200$, $\eta_1 = 0.1$ the drag coefficient under perfect slip is 1/60 of that under nonslip[2], and the surface velocity v_θ (made dimensionless by U) comes quite close to that of potential flow (see Figure 3). The velocity profile normal to the surface at $\theta = \pi/4$, where the η-coordinate coincides with the y-axis in Figure 2, reveals that flow under perfect slip approaches the potential flow away from the body much sooner than flow under nonslip (Figure 4). This indicates, if extrapolation to larger Reynolds number is allowed, that the boundary layer under perfect slip is thinner than that under nonslip.

Blunt bodies or plates perpendicular to the main flow behave differently. As already indicated in the solutions for $Re = 0$, the drag coefficients for motions under perfect slip and under nonslip are of the same order. Figure 5 shows the transient stage of a flow normal to a thin elliptic cylinder. The drag coefficient, which is defined here by $C_D = \text{Drag}/(\rho/2)dU^2$, is plotted against t for $\alpha = 90^{\circ}$, $Re = 10$, $\eta_1 = 0.1$. Only a slight difference between nonslip and perfect slip is observed. The surface velocity, which is plotted in Figure 6, deviates considerably from that of potential flow. The occurrence of a negative velocity in the

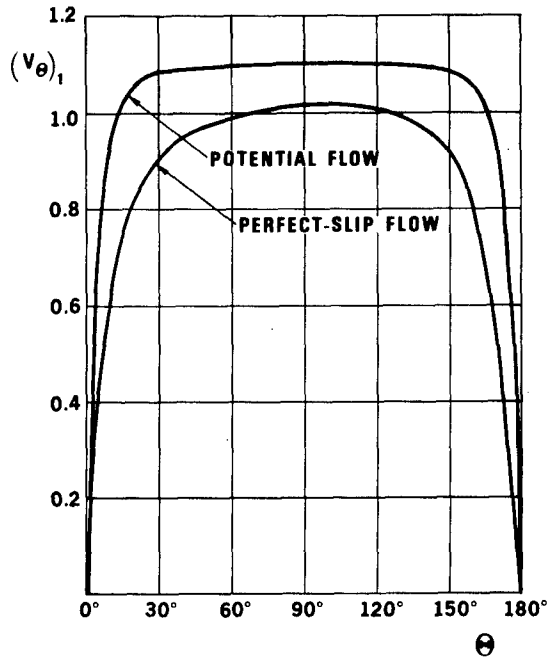

Figure 3. Surface Velocity for $\alpha = 0^{o}$, Re = 200, $\eta_1 = 0.1$ at Almost Steady State

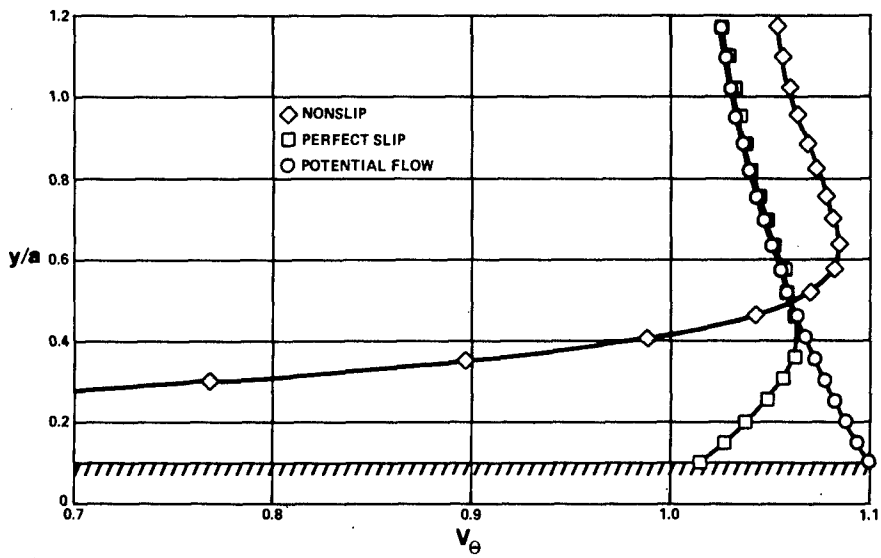

Figure 4. Velocity Profiles for $\alpha = 0^{o}$, Re = 200, $\eta_1 = 0.1$ $\theta = \pi/4$ at Almost Steady State

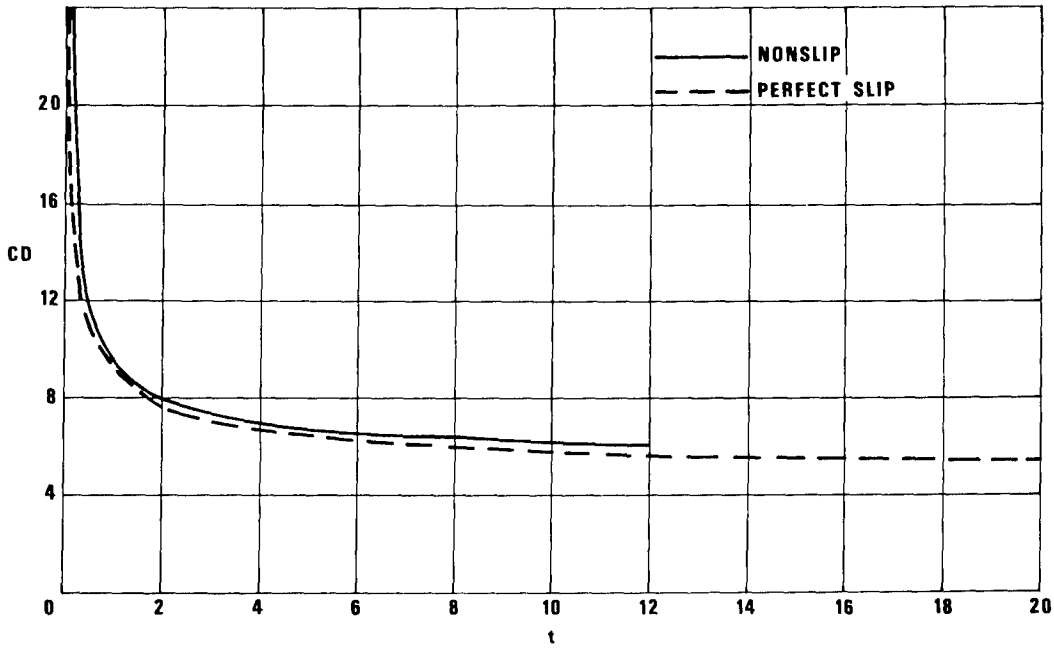

Figure 5. Drag Coefficient Against Time for $\alpha = 90^{O}$, Re = 10, $\eta_1 = 0.1$. Abrupt Start at t = 0.

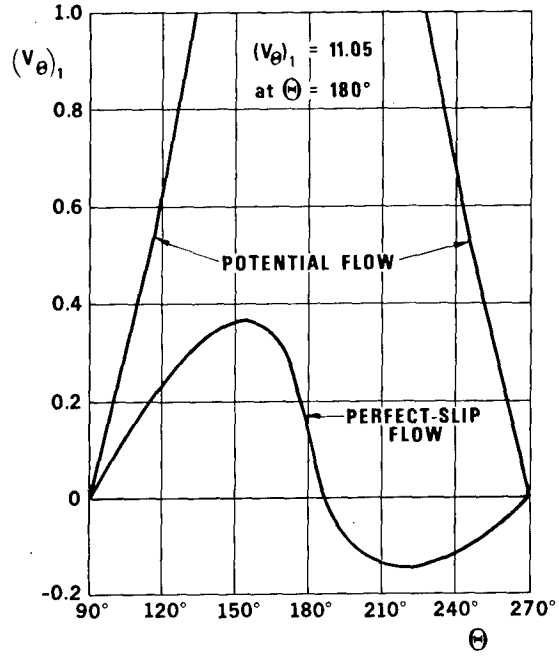

Figure 6. Surface Velocity for $\alpha = 90^{O}$, Re = 10, $\eta_1 = 0.1$ at Almost Steady State

wake points to flow separation, which is verified in Figure 7. Actually, the flow patterns in Figure 7 are almost the same as those for motions under nonslip (see streamline and vorticity patterns[5]). This result is surprising since we expect perfect-slip flow to behave much like potential flow. The development of the wake is recorded in Figure 8, where the dimensionless wake length s'/d is plotted against time. Experimental data from Taneda[6] and Taneda and Honji[7] are included in the graph. Their results are discussed by Lugt and Haussling.[4]

GENERATION OF LIFT UNDER PERFECT SLIP

Classical aerodynamics explains the generation and maintenance of lift of an airfoil by means of the Lanchester-Prandtl hypothesis[8]: After the abrupt start of the body a vortex at the trailing edge develops and separates, leaving behind a bound vortex of equal strength but opposite rotation around the airfoil. Mathematically, a circulation around the airfoil is superposed on the potential-flow solution. This circulation gives rise to a lift force whose magnitude is determined by the Kutta condition at the trailing edge. Since no consideration of viscosity is required in this model (in contrast to the drag force), the nonslip condition of a viscous fluid cannot be applied. The model has been proved to be remarkably good for high Reynolds-number flows. Even for Reynolds numbers as low as 200 the essential features of the model are observed.[4]

If it can be shown that flow under perfect slip satisfies the Kutta condition (in the form extended to viscous fluids), the Lanchester-Prandtl hypothesis must also be valid for perfect-slip flow. The fulfillment of the Kutta condition for perfect-slip flow has been demonstrated[2] for $Re = 200$, $\alpha = 45^{\circ}$. Assuming that this result is valid for higher Reynolds numbers too, we arrive at the important conclusion that the classical airfoil theory is applicable to perfect slip flow. This statement

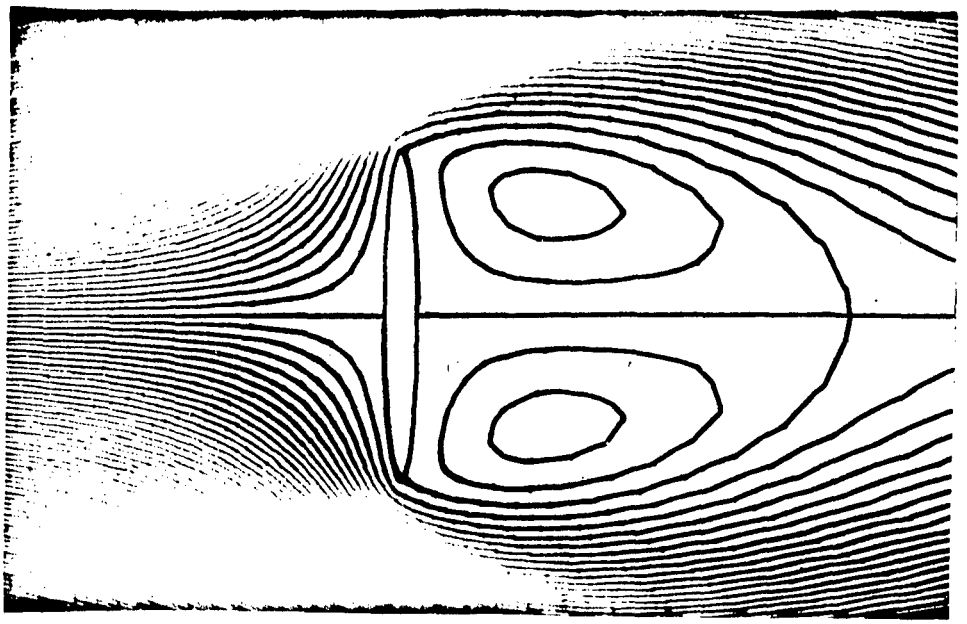

Figure 7. Streamline Patterns for $\alpha = 90^{O}$, Re = 10, $\eta_1 = 0.1$ under Perfect Slip at Almost Steady State.

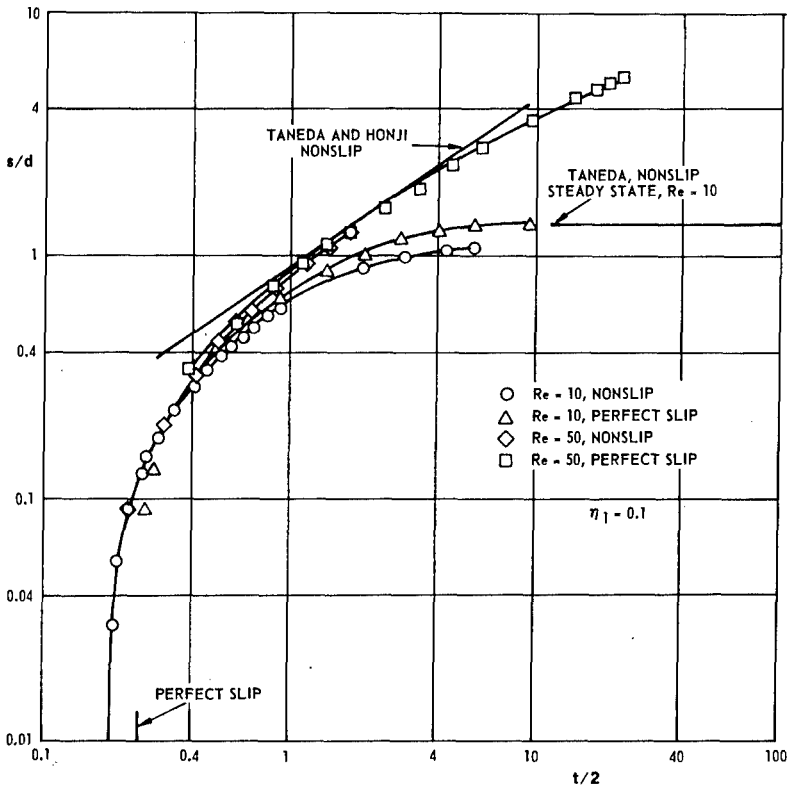

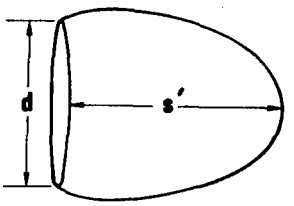

Figure 8. Development of Wake after the Abrupt Start at t = 0. s'/d is Plotted Against t/2.

covers three-dimensional effects since the trailing vortices at the tips of the wings exist also under perfect slip. Thus, an airplane can fly under perfect slip!

Let us consider the initial phase of the process during which the Kutta condition is established and which is not covered by Lugt.[2] The following description holds for both nonslip and perfect slip.

At t = 0 a potential flow around a thin elliptic cylinder for $\alpha = 45^{\circ}$ is assumed without circulation (Figure 9). There is no lift (and no drag). At this instant the initial irrotational disturbance caused by the sudden motion of the body is felt immediately everywhere but vorticity has not yet started to propagate. The generation of a discontinuity sheet for the vorticity on the body surface at t = 0 causes an infinite lift and drag force. Subsequently, the sheet spreads out to a boundary layer, and the lift and drag force drop to finite values.[9] (In Lugt,[2] last paragraph, a difference was reported between perfect slip and nonslip. It was found that the numerical result for perfect slip just after t = 0 is not physically realistic but is the result of the numerical scheme.)

With time inertia carries vorticity from the boundary layer down stream. This causes the rear separation point of the zero streamline to move towards the trailing edge. Thus, the Kutta condition becomes fulfilled at about t = 0.4 (Figure 9). For sufficiently high Reynolds number (observed for Re = 200) the vorticity field forms a local extremum behind the trailing edge which may be interpreted as the starting vortex (Figure 10). However, for Re = 15 and 30 under nonslip, no extremum of the vorticity is observed, although the Kutta condition is satisfied.[4] Diffusion of vorticity dominates here over convection. The Lanchester-Prandtl hypothesis does not hold for this low Reynolds-number flow. It must be emphasized that for all Reynolds numbers the ultimate cause of lift (and drag) is the generation of the vorticity sheet at t = 0.

The streamlines associated with the vorticity extremum are wavy (Figure 9). They represent a vortex moving relative to the reference frame, that is, relative to the body.

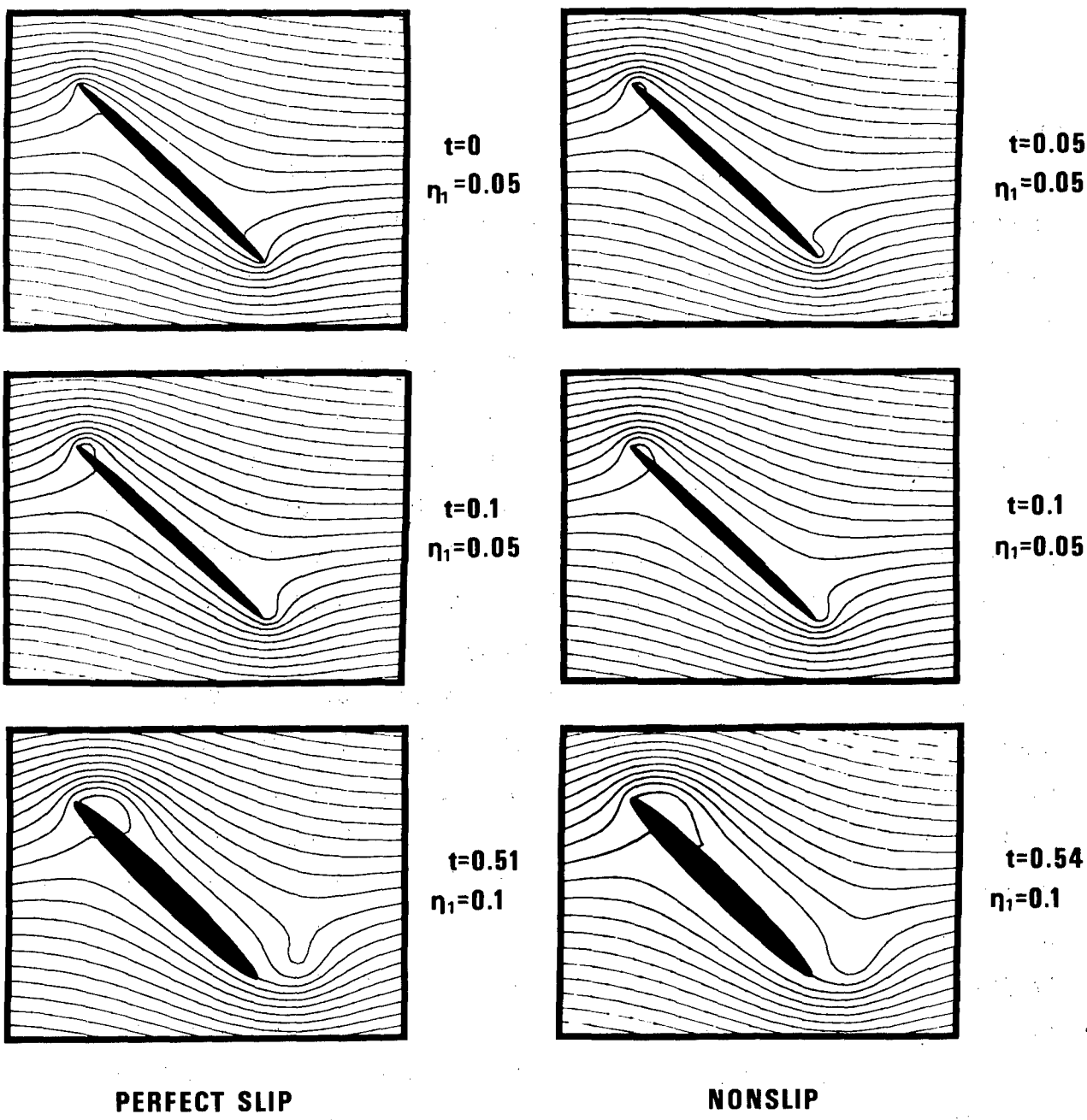

Figure 9. Sequence of Streamline Patterns for $\alpha = 45^{o}$, Re = 200 at Various Times Immediately after the Abrupt Start at t = 0.

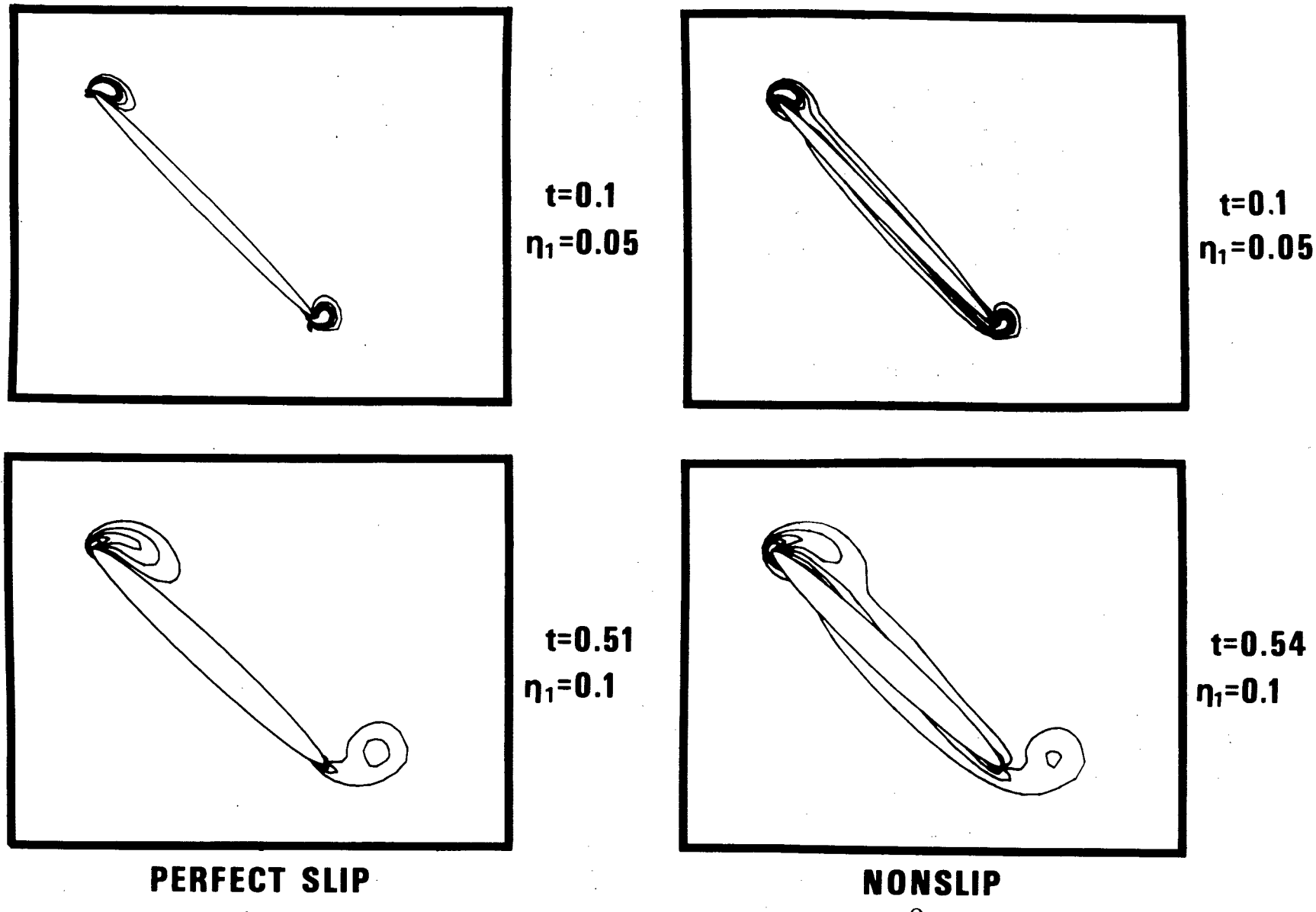

Figure 10. Sequence of Lines of Constant Vorticity for $\alpha = 45^{o}$, Re = 200 at Various Times Immediately after the Abrupt Start at t = 0.

CONCLUSIONS

Perfect-slip flow, if it can ever be approached in reality, differs drastically from nonslip flow when the motion under the nonslip condition is such that the shear stress on the solid wall dominates over the pressure force. Slender bodies parallel to the main stream, fluid motion in capillaries and pipes, and rotating devices such as ball bearings, would benefit most from the slip condition in that drag and pressure loss would be greatly reduced. On the other hand, flows past blunt bodies (and large displacements of fluid in general) are not greatly affected by the change in the surface condition. Classical airfoil theory cannot distinguish between nonslip and perfect slip since the Kutta condition is satisfied for both types of motions. Flow separation, vortex shedding, and instability (which is not explicitly mentioned in this paper, but which precedes vortex shedding) are phenomena which also occur under perfect slip. This implies that turbulent boundary layers at high Reynolds numbers must exist. Turbulence generated away from solid surfaces is, of course, not affected by the slip condition. Turbulence dominates in fluid phenomena in technology and in our every day life. Thus, returning to Goldstein's remark cited in the introduction, that the world would be very different under slippage, perhaps it would be to a certain extent, but not as much as Goldstein might have envisioned. Until perfect-slip flow is verified experimentally, its implications for the world in which we live would make a good subject for science fiction.

ACKNOWLEDGMENTS

The author would like to thank Professor A. Walz from the Technische Universität Berlin for suggesting the subject and for his continued interest in the study. The author also wishes to acknowledge the support of Messrs. H. Haussling and S. Ohring in programming the numerical code.

REFERENCES

[1] S. Goldstein, Fluid Mechanics in the First Half of this Century. Annual Review of Fluid Mechanics, Annual Reviews, Inc., Palo Alto, California; Vol. 1 (1969), 7.

[2] H.J. Lugt, Entstehung und Ausbreitung von Wirbeln unter der "Perfect-Slip" Bedingung. Deutsche Luft-und Raumfahrt Forschungsheft 72-27, Mai 1972. Translated into English in Naval Ship Research and Development Center Report 3794, 1972.

[3] J. Happel, H. Brenner, Low Reynolds Number Hydrodynamics. Prentice-Hall, Inc., Englewood Cliffs, N.J. 1965.

[4] H.J. Lugt, H.J. Haussling, Laminar Flows Past Elliptic Cylinders at Various Angles of Attack. Naval Ship Research and Development Center Report 3748, 1972.

[5] H.J. Lugt, Vortices and Vorticity Around a Moving Plate. Accepted for publication in Scientific American.

[6] S. Taneda, Standing Twin-Vortices behind a Thin Flat Plate normal to the Flow. Research Institute for Applied Mechanics, Kyushu University, XVI, No. 54, 1968, 155.

[7] S. Taneda, H. Honji, Unsteady Flow past a Flat Plate Normal to the Direction of Motion. Journ. Phys. Soc. Japan 30 (1971), 262.

[8] W.F. Durand, Aerodynamic Theory, Dover Publ., New York, 1963, Vol. II, 11.

[9] S.C.R. Dennis, J.D.A. Walker, The Initial Flow Past an Impulsively Started Sphere at High Reynolds Numbers. Journ. Engineering Mathematics 5 (1971), 263.

INITIAL DISTRIBUTION

Copies	
2	U.S. Army Math Res Ctr Univ of Wisconsin, Madison 1 Dr. D. Greenspan 1 Tech Lib
1	U.S. Army Res Off, Durham N. C. 27706 CRD-AA-IPL Box CM
5	CHONR 1 Dr. P. King (102) 1 Mr. M. Cooper (430B) 1 Dr. L.D. Bram (432) 1 Dr. B.J. Macdonald (436) 1 Mr. R.D. Cooper (438)
1	NRL, Tech Lib
1	DNL
2	USNA 1 Dept of Math 1 Tech Lib
4	NAVPGSCOL 1 Lib, Tech Rep Sec 1 Math Dept 1 Dr. T.H. Gawin 1 Prof. T. Sarpkaya
1	NROTC
1	NAVWARCOL
4	NAVSHIPSYSCOM 1 SHIPS 031 1 SHIPS 0311 2 SHIPS 2052
1	NELC, Tech Lib
1	NUC, San Diego, Tech Lib
1	NWC, Tech Lib
3	NOL 1 Dr. R.K. Lobb 1 Dr. G.E. Hudson 1 Tech Lib

Copies	
4	NWL 1 Dr. C.J. Cohen (K) 1 Dr. A.V. Hershey (KXH) 1 Dr. E.W. Schwiderski (KXS) 1 Tech Lib
1	NAVSHIPYD BREM
1	NAVSHIPYD BSN
1	NAVSHIPYD CHASN
1	NAVSHIPYD MARE ISLAND
1	NAVSHIPYD NORVA
1	NAVSHIPYD PEARL
1	NAVSHIPYD PHILA
1	NAVSHIPYD PTSMH
12	DDC
1	NASA HQS
3	NASA Ames 1 Dr. W.J. McCroskey 1 Dr. E.D. Martin 1 Tech Lib
1	NASA Langley
1	NASA Lewis
1	NASA Marshall
1	USAEC, Tech Lib
3	BUSTAND 1 Dr. H. Oser 1 Dr. W. Sadowski 1 Tech Lib
1	Oak Ridge Nat'l Lab
3	Nat'l Ctr for Atmospheric Res, Boulder, Colo. 80301 1 Dr. D.K. Lilly 1 Dr. A. Kasahara 1 Dr. J.W. Deardorff

Copies	
3	Los Alamos Sci Lab, Los Alamos, N.M. 87544 1 Dr. F.H. Harlow 1 Dr. B.J. Daly 1 Tech Lib
2	Brookhaven Nat'l Lab, Upton, L.I., N.Y. 1 Dr. P. Michael 1 Tech Lib
3	Brown Univ, Prov., R.I. 1 Prof. W. Prager 1 Prof. J. Kestin 1 Prof. M. Sibulkin
3	Courant Inst of Math Sci, N.Y.U., N.Y., N.Y. 10012 1 Prof. H.B. Keller 1 Dr. A.J. Chorin 1 Dr. Burstein
2	Harvard Univ 1 Prof. G. Birkhoff 1 Prof. F.G. Carrier
3	Univ of Maryland 1 Prof. A.J. Faller 1 Prof. A. Plotkin 1 Prof. D. Sallet
3	MIT, Cambridge 1 Prof. J.G. Charney 1 Prof. C.C. Lin 1 Prof. S.A. Orszag
1	Univ of Notre Dame 1 Prof. A.A. Szewczyk
2	Poly Inst of Brooklyn 1 Prof. G. Moretti 1 Prof. R.C. Ackerberg
5	Princeton Univ 1 Prof. S.I. Cheng 1 Dr. J. Smagorinsky 1 Dr. K. Bryan 1 Aerospace & Mech Eng Lib 1 Prof. M. Kruskal

Copies	
2	Stanford Univ 1 Prof. A. Acrivos 1 Prof. M.D. Van Dyke
2	West Virginia Univ 1 Prof. J.B. Fanucci 1 Prof. W. Squire
2	Nat'l Sci Foundation 1 Engin Sci Div 1 Math Sci Div
1	Hq., American Soc of Naval Engineers, 1012 14th St., N.W., Wash., D.C. 20005
1	Prof. J.S. Allen Penn St Univ, Dept of Aerospace Eng, Univ Pk, Pa 16802
1	Dr. C.W. van Atta Univ of Calif, La Jolla Calif 92037
1	Dr. J.E. Fromm Dept. 977, Bldg 025, Res. Div, IBM Corp, Monterey and Cottle Road, San Jose, Calif 95114
1	Prof. Raymond E. Goodson Purdue Univ, Automatic Control Ctr, School of Mech Engr, Lafayette, Indiana
1	Prof. J. Happel Dept of Chemical Engin, New York Univ, New York
1	Mr. Stanley K. Jordan The Analytic Sciences Corp 6 Jacob Way Reading, Mass. 01867
1	Prof. M.Z. v.Krzywoblocki Mich St. Univ., East Lansing, Michigan

Copies

1 Prof. Edmund V. Laitone
Div of Aeronautical Sciences
Univ of Calif, Berkeley 94720

1 Dr. W.E. Langlois
IBM Res Lab. San Jose, Calif

1 Prof Z. Lavan
Illinois Inst of Tech
Chicago, Illinois 60616

1 Prof. M.V. Morkovin
Dept Mechanical & Aerospace
Engr., Ill Inst of Tech
Chicago, Illinois 60616

1 Dr. Vivian O'Brien
The Johns Hopkins Univ
APL, 8621 Georgia Ave,
Silver Spring, Maryland 20910

1 Dr. D. Thoman
C23 E. Mishawaha Ave,
Mishawaha, Indiana

1 Prof. K.E. Torrance
Cornell Univ
Ithaca, New York

1 Prof. W.W. Wilmarth
Univ of Mich, 1077 East
Engin Bldg, Ann Arbor, Mich 48104

1 Prof. James C. Wu
School of Aerospace Engr,
Georgia Inst of Tech
Atlanta, Georgia 30332

CENTER DISTRIBUTION

Copies	
1	01
1	15
1	154
1	1541
1	1552
1	16
1	18-1808-1809
1	1802.1
1	1802.2
50	1802.3
1	1802.4
1	1805
1	183
1	184
5	1843
1	185
1	186
1	188
1	189
2	1892
1	19

UNCLASSIFIED
Security Classification

DOCUMENT CONTROL DATA - R & D

(Security classification of title, body of abstract and indexing annotation must be entered when the overall report is classified)

1. ORIGINATING ACTIVITY (Corporate author)	2a. REPORT SECURITY CLASSIFICATION
Naval Ship Research & Development Center Bethesda, Maryland 20034	UNCLASSIFIED
	2b. GROUP

3. REPORT TITLE

Laminar Flow Past Bodies Under Perfect Slip

4. DESCRIPTIVE NOTES *(Type of report and inclusive dates)*

5. AUTHOR(S) *(First name, middle initial, last name)*

Hans J. Lugt

6. REPORT DATE	7a. TOTAL NO. OF PAGES	7b. NO. OF REFS
July 1973	26	9

8a. CONTRACT OR GRANT NO.	9a. ORIGINATOR'S REPORT NUMBER(S)
b. PROJECT NO. Subproject SR 014 03 01	4227
c. Work Unit 1-1843-347	9b. OTHER REPORT NO(S) *(Any other numbers that may be assigned this report)*
d.	

10. DISTRIBUTION STATEMENT

Approved for public release; distribution unlimited.

11. SUPPLEMENTARY NOTES	12. SPONSORING MILITARY ACTIVITY
	Naval Ship Systems Command

13. ABSTRACT

Current experience conducted at Dornier System on special solid-surface treatment have prompted a study on the fluid dynamic implications of perfect-slip flow. Numerical results on incompressible fluid flows past thin elliptic cylinders at various angles of attack and at moderate Reynolds numbers show that flow separation, instability, and vortex shedding occur also under the perfect-slip condition. Of particular interest is the generation and spreading of an initial vortex after the abrupt start of an airfoil. The circulation theory of lift for potential flows is also applicable to perfect slip. Thus, lift exists so that flying under perfect slip is possible.

14 KEY WORDS	LINK A		LINK B		LINK C	
	ROLE	WT	ROLE	WT	ROLE	WT
Perfect Slip Navier-Stokes Equations Vorticity Production						